EARTHQUAKE ENGINEERING AND STRUCTURAL DYNAMICS
Earthquake Engng. Struct. Dyn. **28**, 1525–1540 (1999)

VERTICAL AND ROCKING IMPEDANCES FOR RIGID RECTANGULAR FOUNDATIONS ON SOILS WITH BOUNDED NON-HOMOGENEITY

CHRISTOS VRETTOS*
Technical University of Berlin, Section of Geotechnical Engineering, 10623 Berlin, Germany

SUMMARY

The vertical and rocking response of rigid rectangular foundations resting on a linear-elastic, compressible, non-homogeneous half-space soil model is studied. The non-homogeneity is described by a continuous yet bounded increase of shear modulus with depth. The mixed boundary value problem is solved by means of the semi-analytical method of the subdivision of the foundation/soil contact area whereby the influence functions for the sub-regions are determined by integration of the corresponding surface-to-surface Green's functions for the particular soil model. Impedance functions are given for representative values of the non-homogeneity parameters, the Poisson's ratio and the foundation geometry over a wide range of frequencies. Significant features associated with the soil non-homogeneity are pointed out. Copyright © 1999 John Wiley & Sons Ltd.

KEY WORDS: footings; vibration; soil–structure interaction; impedance; soil non-homogeneity; numerical analysis

INTRODUCTION

For the solution of dynamic soil–structure interaction problems the model of a linear-elastic medium is adopted which is described by means of the two elastic parameters — elastic modulus and Poisson's ratio — and the mass density. Even in non-layered, uniformly deposited strata, however, soil stiffness, expressed in terms of elastic modulus, increases with effective confining pressure and accordingly with depth due to differential compaction effects, while the two other soil parameters, density and Poisson's ratio, do not vary considerably with depth and are taken to be approximately constant. Such a soil medium with a continuous variation of elastic modulus with depth is referred to as 'non-homogeneous'. The effects of non-homogeneity began to be considered in soil–structure interaction, both static and dynamic, soon after Gibson[1] introduced a special type of non-homogeneity with linearly varying elastic modulus with depth in an incompressible half-space with vanishing modulus at the surface, which was used to model water-saturated clays.

* Correspondence to: Christos Vrettos, Philipp Holzmann Planungsgesellschaft mbH, An der Gehespitz 50, Neu-Isenburg, D-63263, Germany

CCC 0098–8847/99/121525–16$17·50

Received 4 September 1998
Revised 28 January 1999
Accepted 22 June 1999

Apart from a few exemptions, boundary value problems involving foundation vibrations in this type of soil media have been treated mainly using numerical methods for multi-layered viscoelastic soils by approximating the continuous variation of soil properties with depth by a stack of homogeneous layers. Wong and Luco[2] used the integral equations approach and the Green's functions reported by Apsel[3] for computing impedance functions for rigid square footings on a layer with linearly increasing wave velocity, bonded to an underlying half-space. The thin-layer method[4,5] was used by Waas *et al.*[6] to determine impedances for circular footings resting on a compressible Gibson soil layer over bedrock. In a more recent work[7] the problem was reconsidered whereby the rigid base was replaced by a half-space approximation.

The lack of analytical solutions is mainly associated with the mathematical difficulties arising from the fact that decoupling of the wave equations of motion, as known from the classical treatment of the case of a homogeneous half-space, is only feasible for specific variations of the elastic modulus, Poisson's ratio and mass density which are not realistic for soils, the only exemption being the aforementioned Gibson soil. For that model Awojobi[8,9] studied the dynamic response of foundations, but only for some asymptotic cases. Another case where decoupling is feasible is that of a linear velocity increase with depth and a Poisson's ratio of 0·25. This model was adopted by Gazetas[10] to investigate the response of strip footings on multi-layered soil consisting of a stack of non-homogeneous layers, and very recently by Guzina and Pak[11] who presented analytical solutions for the vertical response of rigid circular footings on this type of continuously non-homogeneous half-space.

Another class of solutions refers to simple models as used by Gazetas and Dobry[12,13] and Wolf and Meek[14] to estimate dynamic foundation response based on physical insight and calibration with exact solutions. Formulae for circular and strip foundations resting on non-homogeneous soil are summarized by Gazetas,[15] which, however, are only crude approximations and should be used judiciously.

The aforementioned linear-wave-velocity soil corresponds for constant mass density to a soil modulus increase with the square of the depth. Thus, although the solution by Guzina and Pak[11] is of great value as benchmark for numerical codes, this model has little practical significance since it is a well-known fact that irrespective of the nature of sedimentary strata the variation of elastic moduli with effective confining pressure is a sublinear function. In addition to this, the unboundedness of the modulus at infinity, a common feature for all power-law models, is not only the main source of mathematical difficulties but also a physically less meaningful characteristic of the soil model.

Avoiding such constraints the author introduced a compressible elastic half-space model whose modulus varies with depth according to a continuous function which is bounded at infinity and non-zero at the surface to investigate surface wave propagation.[16] The fundamental solution is obtained without the use of potentials by directly solving the associated system of coupled differential equations. For this versatile half-space soil model he then analytically solved the dynamic counterpart of Boussinesq's problem by applying classical integral transform techniques and residue integration.[17] This solution is used in the sequel to derive vertical and rocking impedance functions for rectangular foundations using the semi-analytical method of subdivision of the contact area foundation/soil. Selected numerical results are presented demonstrating the influence of non-homogeneity, Poisson's ratio and base aspect ratio on foundation response. The corresponding static solution of the soil–structure interaction problem treated herein has been presented very recently by the author.[18]

METHOD OF ANALYSIS

Consider a rigid massless rectangular foundation with side lengths $2b$ and $2a$ with $b \geqslant a$ resting on the surface of a linear-elastic, isotropic half-space of constant mass density ϱ and Poisson's ratio v, with $0 \leqslant v < 0{\cdot}5$, and shear modulus G varying with depth z such that

$$G(z) = G_0 + (G_\infty - G_0)(1 - \mathrm{e}^{-\alpha z}) \tag{1}$$

where G_0 and G_∞ are the shear moduli at the surface and at infinite depth, respectively, and α is a constant with dimension of inverse length which is referred to as non-homogeneity gradient. The foundation is loaded at its centre by a harmonic vertical load $P\mathrm{e}^{\mathrm{i}\omega t}$ and harmonic moments $M_y\mathrm{e}^{\mathrm{i}\omega t}$ and $M_x\mathrm{e}^{\mathrm{i}\omega t}$ about the long and short foundation axis, resp., as depicted in Figure 1, whereby ω is the circular frequency, i is the imaginary unit and t denotes time.

The contact between the soil and the foundation is assumed frictionless. The method adopted for solving the mixed boundary value problem consists in subdiving the contact area in a finite number of uniformly loaded rectangular elements and imposing the rigid body translation or rotation condition for determining the unknown complex valued stress magnitude at each element.[19–21] The complex valued influence function relating the vertical displacement at the centre of any of the elements due to a uniform vertical stress applied at another element is obtained by integration of the surface-to-surface harmonic Green's function, i.e. the response of the half-space to a unit harmonic surface load. For the particular non-homogeneous soil model considered herein this solution has been presented by the author.[17] The vertical surface displacement w due to a vertical harmonic point load $Q\mathrm{e}^{\mathrm{i}\omega t}$ is given in dependency on the circular frequency ω and the distance from the source r as

$$w(\omega, r) = \frac{Q}{G_0 r}\,\tilde{F}_{zz}(\bar{\omega}, v, \Xi_0, \bar{\theta}) \tag{2}$$

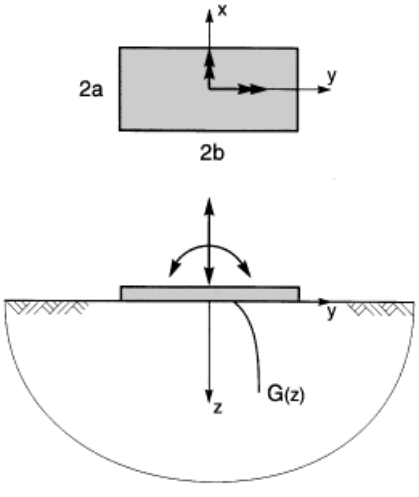

Figure 1. The problem under consideration

In this expression $\tilde{F}_{zz}$ is a complex-valued function and

$$\bar{\omega} = k_{s0} r \tag{3}$$

is a dimensionless frequency parameter (or equivalently a dimensionless distance parameter) where

$$k_{s0} = \frac{\omega}{v_{s0}} \tag{4}$$

is the wave number of the shear wave at the surface with

$$v_{s0} = \sqrt{\frac{G_0}{\varrho}} \tag{5}$$

denoting the shear wave velocity at the soil surface. The effects of non-homogeneity are represented in equation (2) by the degree of non-homogeneity Ξ_0 with

$$\Xi_0 = 1 - \frac{G_0}{G_\infty} \tag{6}$$

and by the dimensionless non-homogeneity gradient $\bar{\theta}$ with

$$\bar{\theta} = \frac{k_{s0}}{\alpha} \tag{7}$$

The case $0 \leqslant \Xi_0 < 1$ ($G_0 \leqslant G_\infty$) will be considered here. For given Ξ_0 and ν, the function $\tilde{F}_{zz}$ describes by means of two dimensionless variables the relationship between the three characteristic lengths of the boundary value problem of a point load on the soil surface, i.e. the distance from the source r, the inverse non-homogeneity gradient α^{-1} and the inverse wave number of the shear wave at the surface k_{s0}^{-1} (wavelength of shear wave at the surface divided by 2π). Thus, instead of $\bar{\omega}$ and $\bar{\theta}$ one may introduce $\bar{r} = r\alpha$ and use the equivalent sets $\bar{r}$ and $\bar{\omega}$ or $\bar{r}$ and $\bar{\theta}$, resp.

The limiting case of a homogeneous soil with shear modulus G_0 is recovered either when $\Xi_0 = 0$ or as $\bar{\theta} \to \infty$, which implies $\alpha \to 0$.[17]

Influence functions for the rectangular elements are computed by numerical integration of the surface-to-surface Green's function, equation (2), using standard Gauss–Legendre quadrature. The most critical point of the integration is the computation of the influence function for the loaded element itself due to the singularity of the Green's function at the origin. Details of the integration procedure are presented in the appendix.

The influence function for the loaded element corresponds to the half-space response to a uniform harmonic surface load $q e^{i\omega t}$ acting over a rectangular area of the dimensions of the element $2a \times 2b$ with $b \geqslant a$. The vertical displacement at the centre of the loaded area w_A is computed next. For given values of the Poisson's ratio ν, of the degree of non-homogeneity Ξ_0 and of the aspect ratio b/a, the solution for w_A is expressed in terms of the following two parameters:

The dimensionless frequency

$$a_0 = \frac{\omega a}{v_{s0}} = k_{s0} a \tag{8}$$

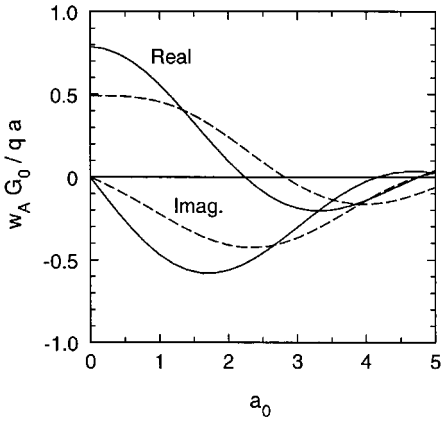

Figure 2. Complex central displacement of a square uniform load $qe^{i\omega t}$ on homogeneous soil (solid line) and non-homogeneous soil with $\Xi_0 = 0{\cdot}5$ and $\bar{\alpha} = 1$ (dashed line). Poisson's ratio $\nu = 0{\cdot}3$

and the dimensionless non-homogeneity gradient

$$\bar{\alpha} = a\alpha \tag{9}$$

which relates the half-width of the loaded area a to the non-homogeneity gradient α.

Each pair $(\bar{\alpha}, a_0)$ corresponds to a single value $\bar{\theta}$, since by combining equations (7) and (8) it follows

$$\bar{\theta} = \frac{a_0}{\bar{\alpha}} \tag{10}$$

This means that for given Ξ_0 and ν the Green's functions for given $\bar{\theta}$ can be used in the solution of the boundary value problem for any combination of a_0 and $\bar{\alpha}$ which fulfils equation (10).

The accurate determination of the soil response in the neighbourhood of the static solution, i.e. for small values a_0, requires the value of the Green's function at the origin. A convergence study shows, that for all values Ξ_0 and $\bar{\theta}$ as $\bar{\omega} \to 0$ the real part of the normalized Green's function wrG_0/Q reaches the static solution for the homogeneous half-space, $(1 - \nu)/2\pi$, while the imaginary part disappears. The effects of non-homogeneity on the half-space response become apparent as the distance from the source increases, or, in other words, at small distances from the load the half-space region contributing to the surface displacement is confined near the surface.

Figure 2 depicts the real and the imaginary part of the normalized central displacement of a square uniform load $qe^{i\omega t}$ in dependency on the dimensionless frequency a_0 for $\nu = 0{\cdot}3$, $\Xi_0 = 0{\cdot}5$ and $\bar{\alpha} = 1$. For comparison the curves of the homogeneous half-space are also given. As $a_0 \to 0$ the real part reaches the corresponding static solution, while the imaginary part disappears. The static solution[18] yields for $\Xi_0 = 0{\cdot}5$ a value $w_A G_0/qa = 0{\cdot}4909$ whereas for the homogeneous case ($\Xi_0 = 0$) the respective value is $w_A G_0/qa = 0{\cdot}7855$.

NUMERICAL RESULTS AND DISCUSSION

Making use of the lumped parameter concept the complex valued, frequency-dependent force–displacement and moment–rotation relationships of the rigid foundation $\mathscr{K}_j$, termed impedance

functions, are introduced as

$$\mathscr{K}_j = \tilde{K}_j + \mathrm{i}\omega C_j \tag{11}$$

where $j = zz$ for vertical vibration and $j = ry$ and $j = rx$ for rocking vibration about the long and the short axis of the foundation, resp. $\tilde{K}_j(\omega)$ is the dynamic stiffness and $C_j(\omega)$ is the radiation dashpot coefficient.

The accuracy of the numerical method described above depends markedly on the discretization degree of the contact area. In order to take advantage of the symmetry, quadratic contact elements are used whereby N denotes the number of elements in the direction of the shorter side of the foundation. The required degree of discretization depends on the frequency range considered. For the present study $N = 10$ was selected. Comparison of the limiting case of the homogeneous soil ($\Xi_0 = 0$) to the results by Wong and Luco[19] and Sarfeld[21] obtained by the same method shows excellent agreement. An additional check against the static foundation stiffness for the non-homogeneous soil model[18] yields identical values as $\omega \to 0$.

The performance of the numerical method is further demonstrated in a recent paper by the author[22] where the influence of non-homogeneity on the static contact stress distribution is investigated by using two different schemes for the discretization of the foundation/soil contact area. For the present paper static and dynamic contact stress distribution have been checked against the results by Gaul[23] for homogeneous soil showing excellent agreement.

In the customary representation of the impedance functions both the dynamic stiffness and the dashpot coefficient in equation (11) are normalized with respect to the static stiffness while the frequency dependency is expressed by the dimensionless frequency a_0 according to equation (8). As will be shown, in non-homogeneous soil the normalization with respect to the static stiffness is meaningful only for the dynamic stiffness $\tilde{K}_j$. The normalization of the radiation dashpot coefficient C_j is made in terms of the radiation impedance (damping per unit contact area) $\varrho\hat{v}$, as suggested by Gazetas and Dobry,[12] whereby $\hat{v}$ is an appropriate wave velocity. For vertical translation the resulting dimensionless parameter is $C_{zz}/\varrho\hat{v}A$, with A being the foundation-soil contact area, while for rocking motion the area A is replaced by the contact-area moment of inertia around horizontal axes I_{ry} and I_{rx}. These authors defined $\hat{v}$ to be a ficticious velocity so as to yield for vertical vibrations at the high-frequency limit a value $C_{zz}/\varrho\hat{v}A \to 1$. However, at high frequencies and for values of the Poisson's ratio near the incompressibiliy limit $v = 0{\cdot}5$ their formula is only a rough approximation.

In an alternative approach we define the velocity $\hat{v}$ so as to yield for vertical vibration a value of about 1 near the low-frequency limit $a_0 \to 0$ by introducing

$$\hat{v} = \frac{v_{\mathrm{S}0}}{1 - v} \tag{12}$$

Based on this, the following normalization is selected for the dynamic stiffness and dashpot coefficient:

$$\tilde{K}_j = K_j k_j \quad (j = zz, ry, rx) \tag{13}$$

where K_j denotes the static foundation stiffness, and

$$C_{zz} = \varrho\hat{v}Ac_{zz} \tag{14}$$

$$C_j = \varrho\hat{v}I_j c_j \quad (j = ry, rx) \tag{15}$$

For the rectangular foundation: $A = 4ab$, $I_{ry} = (4/3)\ ba^3$, and $I_{rx} = (4/3)ab^3$.

Numerical values for the static stiffnesses K_j are summarized for the cases considered next in Table I. Note that $N = 10$ is used throughout the paper in contrast to Reference 18 where values for $N \to \infty$ for the static case are obtained by extrapolation from results at different discretization degrees of the contact area. In Reference 18 it is shown that the term $(1 - \nu)$ can approximately describe the dependence of K_j on the Poisson's ratio.

The suitability of the proposed normalization for the radiation dashpot coefficients c_j in homogeneous soil is demonstrated in Figure 3 for a square foundation and for three different values of the Poisson's ratio. Over a wide frequency range of interest in practice the curves for vertical vibration almost coincide. The curve for $\nu = 0{\cdot}45$ starts to diverge as soon as a certain frequency is reached, while for the rocking motion curve deviation continuously increases with frequency. If can thus be infered that at higher frequencies and as ν approaches the incompressibility limit the factor $(1 - \nu)$ can not satisfactorily describe the dependency on Poisson's ratio, whereby the vertical translation mode is more sensitive than the rocking mode.

Figure 4 shows for $\Xi_0 = 0{\cdot}5$ and $\nu = 0{\cdot}3$ the influence of the dimensionless non-homogeneity gradient $\bar{\alpha}$ on the vertical and rocking impedances of a square foundation while Figure 5 depicts the corresponding curves for a soil with a stronger non-homogeneity given by $\Xi_0 = 0{\cdot}7$ and $\Xi_0 = 0{\cdot}9$. Larger values than $\Xi_0 = 0{\cdot}9$, which corresponds to $G_\infty/G_0 = 10$, are not likely to be physically meaningful. Results for a rectangular foundation with aspect ratio $b/a = 2$ and $b/a = 4$ are

Table I. Static stiffnesses for rigid rectangular foundations

Ξ_0	ν	$\bar{\alpha}$	b/a	K_{zz}/G_0a	K_{ry}/G_0a^3	K_{rx}/G_0a^3
0·0	0·3		1	6·373	5·370	5·370
			2	9·326	9·610	27·044
			4	14·277	17·992	144·047
0·0	0·2		1	5·576	4·699	4·699
	0·45			8·111	6·835	6·835
0·5	0·3	0·5	1	9·188	6·508	6·508
			2	14·113	11·842	35·174
			4	22·556	22·422	201·029
0·5	0·3	1·0	1	10·115	7·180	7·180
		1·5		10·636	7·653	7·653
0·5	0·2	0·5	1	7·908	5·630	5·630
		1·0		8·694	6·183	6·183
0·5	0·45	0·5	1	12·154	8·507	8·507
		1·0		13·420	9·486	9·486
0·7	0·3	0·25	1	10·469	6·824	6·824
		0·5		12·314	7·812	7·812
		1·0		14·458	9·246	9·246
0·9	0·3	0·1	1	13·092	7·600	7·600

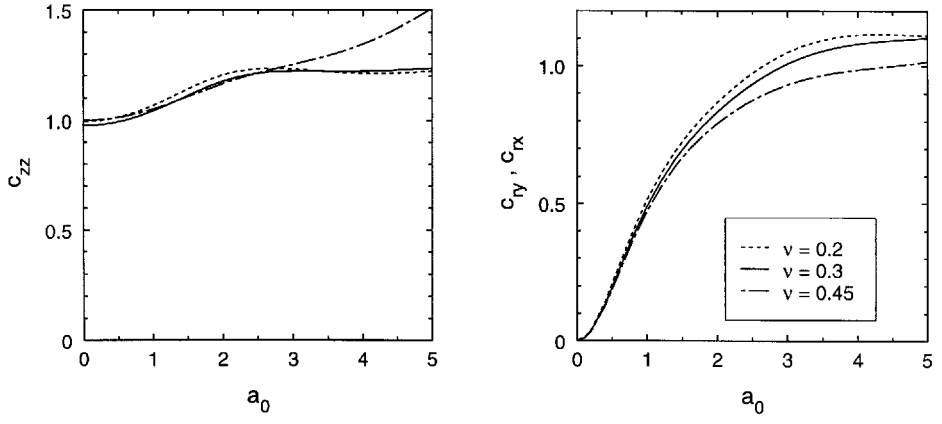

Figure 3. Normalized radiation dashpot coefficients for square foundation on homogeneous soil for three values of the Poisson's ratio v

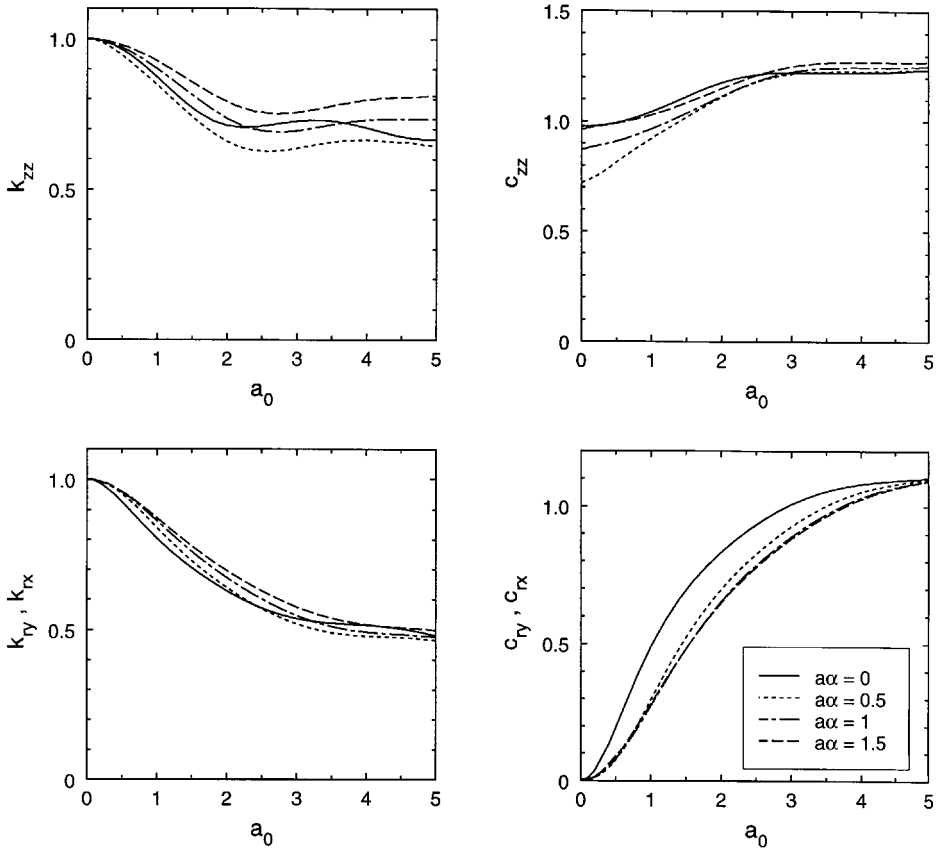

Figure 4. Normalized dynamic stiffness and radiation dashpot coefficients for vertical and rocking motion of a square foundation on non-homogeneous soil with $\Xi_0 = 0{\cdot}5$ and different values $\bar{\alpha} = a\alpha$. Poisson's ratio $v = 0{\cdot}3$

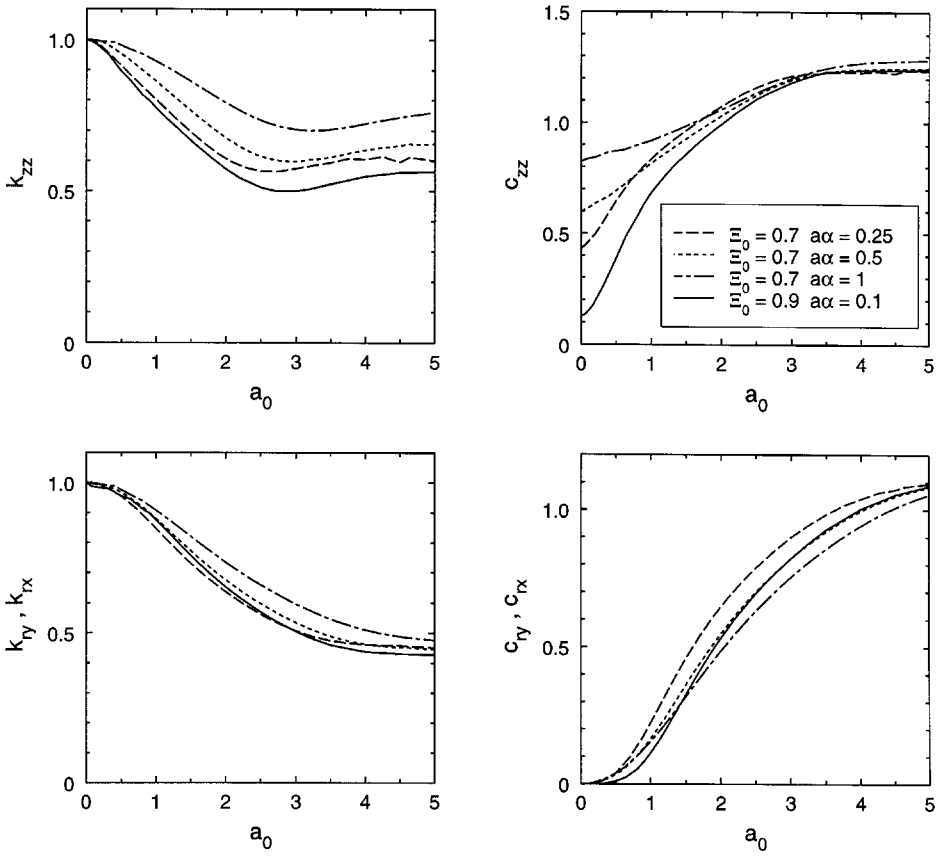

Figure 5. Normalized dynamic stiffness and radiation dashpot coefficients for vertical and rocking motion of a square foundation on non-homogeneous soil for different values Ξ_0 and $\bar{\alpha} = a\alpha$. Poisson's ratio $\nu = 0{\cdot}3$

plotted in Figure 6 for $\Xi_0 = 0{\cdot}5$. Curves for non-homogeneous soil are contrasted with the corresponding curves for homogeneous soil.

Regarding the dynamic stiffness coefficients $k_j(a_0)$ the following characteristics are worthy of note in Figures 4–6:

(i) Non-homogeneity mainly affects the vertical and to a much lesser extent the rocking vibration mode. This can be explained by the fact that the vertical vibration mode reaches deeper half-space regions and the foundation response reflects the broader variation in soil stiffness within the respective region.

(ii) For given Ξ_0 and foundation geometry, an increase of the non-homogeneity gradient α yields a slower decrease of k_j with frequency. While in strongly non-homogeneous soils, e.g. soils with an unbounded quadratic modulus variation, k_j values are always smaller than those for homogeneous soil,[11] this trend no longer holds when the modulus variation becomes bounded.

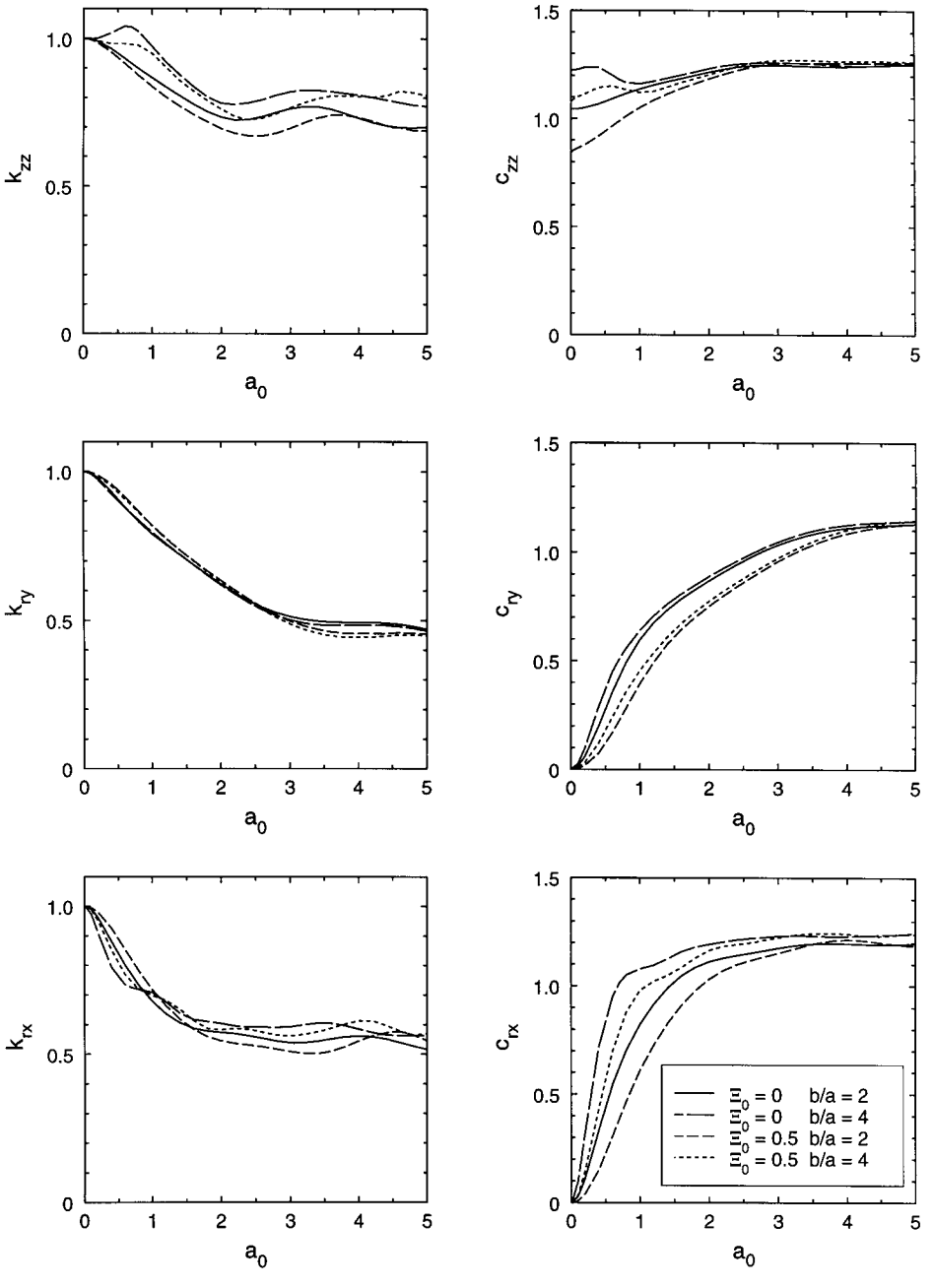

Figure 6. Normalized dynamic stiffness and radiation dashpot coefficients for vertical and rocking motion of a rectangular foundation for two values of the aspect ratio b/a. For the non-homogeneous soil $\Xi_0 = 0{\cdot}5$ and $\bar{\alpha} = 0{\cdot}5$. Poisson's ratio $\nu = 0{\cdot}3$

(iii) For week to moderate non-homogeneity degrees, variations in the foundation aspect ratio b/a both for the vertical and for rocking impedances follow the same basic trends as in the homogeneous case so that the approximation $k_j(\Xi_0) \approx k_j(\Xi_0 = 0)$ may be used for practical purposes.

Significant features of the radiation dashpot coefficient curves $c_j(a_0)$ are summarized next.

(i) Non-homogeneity may lead to a reduction of radiation damping compared to a homogeneous soil of shear modulus G_0 in spite of the greater soil stiffness, a fact that is attributed to the rebound of energy caused by continuous reflection of the wave rays.[15] However, this is not invariably true, as shown in Figures 4–6. It is possible that above a certain value $\bar{\alpha}$ or/and frequency a_0 the damping increasing effects attributed to the higher soil stiffness outweigh the damping reducing effects of non-homogeneity, i.e. the number of reflections is not sufficiently large to reduce overall radiation damping compared to that of a homogeneous soil of shear modulus G_0.

(ii) Particular attention deserves the vertical dashpot coefficient c_{zz} at the low-frequency range. For a given foundation geometry c_{zz} decreases as the non-homogeneity becomes stronger (Ξ_0 increases) or as the modulus gradient α decreases. A decrease of α for given Ξ_0 implies that the depth at which G_∞ is asymptotically reached increases so that the soil region in which waves emanating from the foundation undergo reflection becomes larger leading to a reduction of radiation damping. For very low values α or/and high values Ξ_0 the dashpot coefficient c_{zz} tends to zero as $a_0 \to 0$ accompanied by a steep increase of the $c_{zz}(a_0)$ curves near the origin. The trend that lower values α yield less radiation damping may be reversed as soon as a threshold frequency is reached, cf. the two curves for $\Xi_0 = 0{\cdot}7$ in Figure 5.

(iii) At the high-frequency limit all curves tend to the corresponding curves of the homogeneous soil with shear modulus G_0. Evidently, because at high frequencies the motion is confined to a region near the soil surface. As the degree of non-homogeneity increases, this asymptotic behaviour is shifted to higher frequencies.

(iv) Although at low and intermediate frequencies the normalized vertical dashpot coefficient increases as the aspect ratio becomes larger, the asymptotic values for different aspect ratios do not considerably differ, a fact that supports the choice of the normalization used herein, as suggested by Gazetas and Dobry,[12] provided that the Poisson's ratio is sufficiently smaller than 0·5, e.g. $\nu \leqslant 0{\cdot}4$. This trend is also valid for rocking motion whereby the quality of the approximation is better for rocking about the long than about the short foundation axis.

(v) It is apparent, that a normalization of the dashpot coefficient in terms of the corresponding static foundation stiffness, as usually made for the case of homogeneous soil, is inappropriate for non-homogeneous soil since this would shift the dashpot curves downwards and the differences to the homogeneous soil curves would become essentially greater.

(vi) Looking at the rotational dashpot coefficients c_{ry} and c_{rx} in Figure 5 the existence of cut-off frequencies is apparent. For given aspect ratio, the occurrence of this phenomenon requires a combination of a sufficiently large value Ξ_0 with a sufficiently low value $\bar{\alpha}$. Similar behaviour has been reported by Guzina and Pak[11] for the linear-wave-velocity half-space model and for vertical vibration whereby in that model the appearance of cut-off frequencies is more pronounced due to the extremely strong nonhomogeneity.

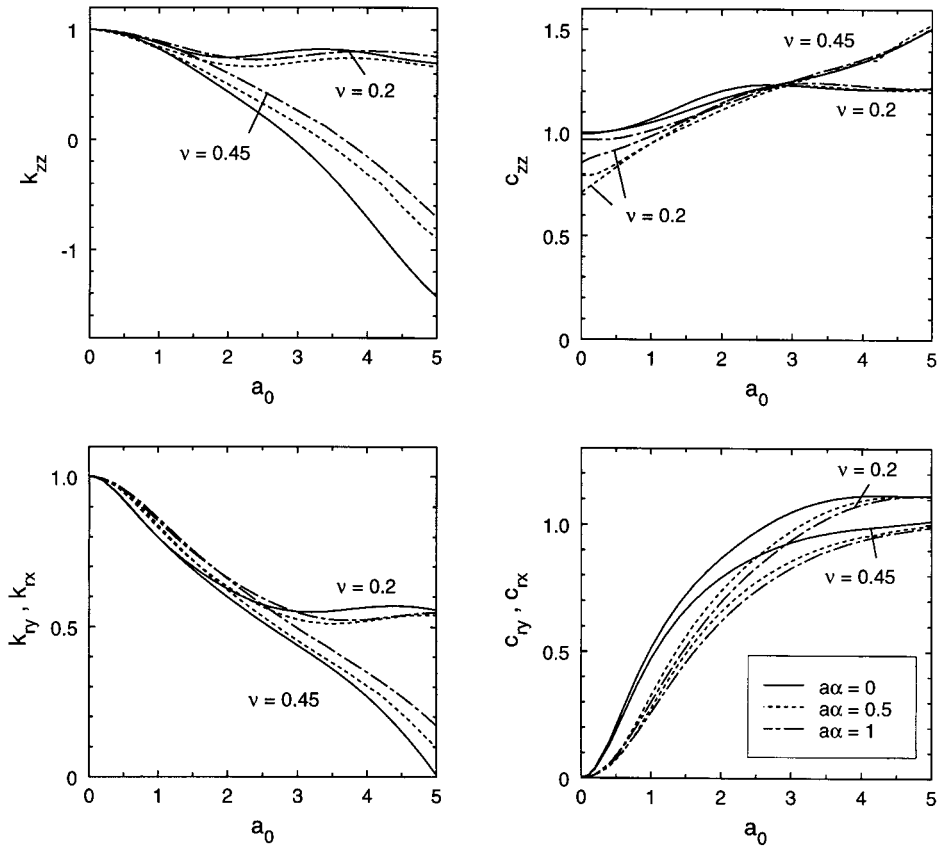

Figure 7. Influence of Poisson's ratio v on normalized dynamic stiffness and radiation dashpot coefficients for vertical and rocking motion of a square foundation on non-homogeneous soil with $\Xi_0 = 0{\cdot}5$ and for three values $\bar{\alpha} = a\alpha$

Figure 7 manifests the strong influence of the Poisson's ratio v on the response of a square foundation as v approaches the incompressibility limit. The frequency at which the curves for $v = 0{\cdot}45$ start to deviate increases with increasing $\bar{\alpha}$ for the rocking stiffness, while the curves for the vertical stiffness differ from each other throughout the entire frequency range. For the vertical radiation dashpot, on the other hand, the frequency at which deviation starts as well as the value of the dashpot coefficient itself beyond this frequency is almost independent of the dimensionless gradient $\bar{\alpha}$.

As mentioned above, k_j and c_j contain in an implicit and in an explicit form, resp., the normalization factor $(1 - v)$. Looking at the dashpot coefficients in Figure 7 it can be seen that the general trend that the curves for $v = 0{\cdot}20$ yield lower values compared to those for $v = 0{\cdot}45$ is reversed for c_{zz} at higher frequencies. Further, it can be deduced that at the low frequency limit the use of the factor $(1 - v)$ for normalization of the vertical dashpot coefficient becomes less appropriate as the non-homogeneity gradient α increases.

Often, in engineering practice one applies the concept of 'equivalent homogeneous soil' by selecting, in dependence on the vibration mode and the foundation geometry, a soil modulus value at a particular depth and using the respective impedance functions of the homogeneous soil model.

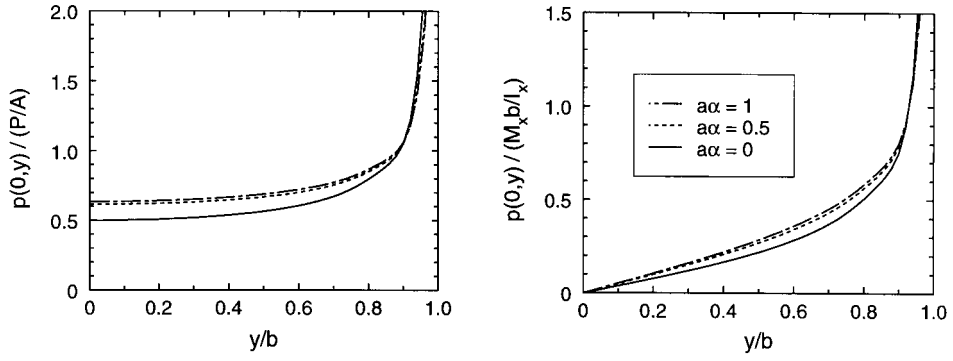

Figure 8. Normalized contact stresses for static vertical and moment loading of a square foundation. The solid line is for homogeneous soil, the dashed lines for non-homogeneous soil with $\Xi_0 = 0{\cdot}7$. Poisson's ratio $\nu = 0{\cdot}3$

While this concept works well for surface wave propagation,[16] it is rather complicated when dealing with dynamic foundation loading. This is due to the fact that the modulus increase with depth leads to an increase of the foundation stiffness and at the same time to a reduction of the radiation damping. Thus, different values have to be used for dynamic stiffness and dashpot coefficients which complicates matters. Waas *et al.*[7] derived such approximate expressions for circular foundations on linearly non-homogeneous soil.

Since the influence of non-homogeneity on the dynamic stiffness coefficients k_j is not strong it is recommended to apply the concept of equivalent homogeneous soil only to the static foundation stiffness K_j. The corresponding equations for the soil model considered herein have been presented in a recent paper by the author[18] and cover wide ranges of the parameters involved.

For the radiation damping coefficient it is recommended to use the curves with the normalization chosen herein and refrain from deriving equivalent homogeneous soil models since for moderate values of the non-homogeneity the discrepancy between the two types of medium is not as severe as it might be expected, and tends to become negligible at higher frequencies. Particular attention should be paid to low frequencies, especially for the vertical vibration mode.

A further point of interest to engineering analysis is the influence of soil non-homogeneity on the distribution of the contact stress $p(x, y)$. Curves for the normalized contact stresses along the axis of symmetry of a square foundation for vertical and moment loading are plotted in Figure 8 for the static case while Figure 9 depicts real and imaginary part of the corresponding solution at a dimensionsless frequency $a_0 = 3$. Results have been obtained for a constant discretization scheme with $N = 25$. It can be seen that for the static case the distribution becomes more uniform as the non-homogeneity increases. For vertical dynamic loading the influence of frequency is more pronounced in the case of homogeneous soil. Finally, the imaginary part for moment loading is considerably more sensitive to variations in the soil non-homogeneity than its vertical loading counterpart.

CONCLUSIONS

Vertical and rocking impedances have been presented for rigid rectangular foundations on a compressible half-space with shear modulus increasing with depth according to a function

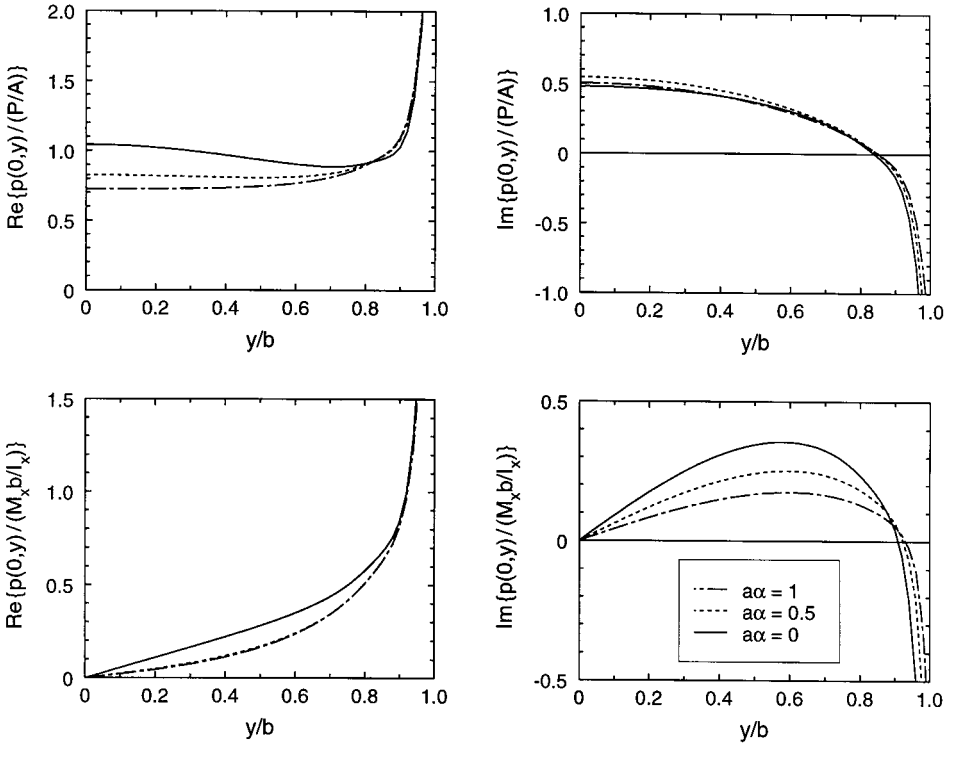

Figure 9. Real and imaginary parts of normalized contact stresses for vertical and moment loading of a square foundation at a dimensionless frequency $a_0 = 3$. The solid line is for homogeneous soil, the dashed lines for non-homogeneous soil with $\Xi_0 = 0{\cdot}7$. Poisson's ratio $\nu = 0{\cdot}3$

which is bounded at infinity. The three parameters of the modulus depth-function can be used to model a variety of real life soil conditions. The introduction of dimensionless quantities encompassing all parameters of the boundary value problem facilitates the identification of the characteristic features associated with non-homogeneity. The method can be extended to treat foundations of arbitrary shape as well as of finite rigidity. Finally, the numerical results presented may be used as benchmarks for numerical codes involving discrete soil models.

APPENDIX

Consider a square of side length $2a$ on the surface of the non-homogeneous soil half-space treated herein and subjected to a uniform vertical load of magnitude q. The complex valued vertical surface displacement at its cental point A is denoted by w_A and is obtained by integration of equation (2). The square is divided into four equal triangles through the point A. The axes of symmetry of the triangles coincide with the x- and y- axis, resp. The vertical surface displacement

at the corner A of the triangle having the y- axis as axis of symmetry is

$$w_A^{(1)} = \frac{q}{G_0} \int_0^a \int_{-x}^{x} \frac{\tilde{F}_{zz}(\bar{\omega})}{\sqrt{x^2 + y^2}} \, \mathrm{d}y \, \mathrm{d}x \tag{16}$$

where $\bar{\omega} = k_{S0}\sqrt{x^2 + y^2}$ is defined by equation (3).

Transformation into polar coordinates (r, ϕ) with $r = \sqrt{x^2 + y^2}$ and $\mathrm{d}y \, \mathrm{d}x = r \, \mathrm{d}\phi \, \mathrm{d}r$ yields the following non-singular expression:

$$w_A^{(1)} = \frac{q}{G_0} \int_{-\pi/4}^{\pi/4} \int_0^{a/\cos\phi} \tilde{F}_{zz}(\bar{\omega}) \, \mathrm{d}r \, \mathrm{d}\phi \tag{17}$$

This integral is subsequently transformed into a Gauss coordinate system $[-1, +1]$ by using

$$r = \frac{a(r^\star + 1)}{2\cos[\phi^\star \pi/4]}, \quad \phi = \phi^\star \pi/4 \tag{18}$$

yielding

$$w_A^{(1)} = \frac{qa}{G_0} \frac{\pi}{8} \int_{-1}^{1} \int_{-1}^{1} \frac{\tilde{F}_{zz}(\bar{\omega})}{\cos[\phi^\star \pi/4]} \, \mathrm{d}r^\star \, \mathrm{d}\phi^\star \tag{19}$$

which is evaluated numerically in a straightforward manner using standard Gauss–Legendre quadrature.

The surface displacement at the cental point A of the square is finally obtained by superposition as

$$w_A = 4w_A^{(1)} \tag{20}$$

REFERENCES

1. R. E. Gibson, 'Some results concerning displacements and stresses in a non-homogeneous elastic half-space', *Géotechnique* **17**, 58–67 (1967).
2. H. L. Wong and J. E. Luco, 'Tables of impedance functions for square foundations on layered media', *Soil Dyn. Earthquake Engng.* **4**, 64–81 (1985).
3. R. J. Apsel, 'Dynamic Green's functions for layered media and applications to boundary value problems', *Ph.D. Thesis*, University of California, San Diego, 1979.
4. G. Waas, 'Linear two dimensional analysis of soil dynamics problems in semi-infinite layered media', *Ph.D. Thesis*, University of California, Berkeley, 1972.
5. E. Kausel, 'An explicit solution for the Green's functions for dynamic loads in layered media', *Research Report R81-13*, *Publ. No. 699*, Dept. of Civil Engineering, MIT, Cambridge, MA, 1981.
6. G. Waas, H. R. Riggs and H. Werkle, 'Displacement solutions for dynamic loads in transversely-isotropic stratified media', *Earthquake Engng. Struct. Dyn.* **13**, 173–193 (1985).
7. G. Waas, H.-G. Hartmann and H. Werkle, 'Damping and stiffness of foundations on inhomogeneous media', *Proc. 9th World Conf. Earthquake Engng., Tokyo*, 1988, Vol. III, pp. 343–348.
8. A. O. Awojobi, 'Vertical vibration of a rigid circular foundation on Gibson soil', *Géotechnique* **22**, 333–343 (1972).
9. A. O. Awojobi, 'Vibration of rigid bodies on nonhomogeneous semi-infinite elastic media', *Quart. J. Mech. Appl. Math.* **26**, 483–498 (1973).
10. G. Gazetas, 'Static and dynamic displacements of foundations on heterogeneous multilayered soils', *Géotechnique* **30**, 159–177 (1980).
11. B. B. Guzina and R. Y. S. Pak, 'Vertical vibration of a circular footing on a linear-wave-velocity half-space', *Géotechnique* **48**, 159–168 (1998).
12. G. Gazetas and R. Dobry, 'Simple radiation damping model for piles and footings' *J. Engng. Mech. Div. ASCE* **110**, 931–956 (1984).
13. G. Gazetas, 'Rocking of strip and circular footings' in D. E. Beskos, T. Krauthammer and I. Vardoulakis (eds), *Proc. Int. Symp. Dynam. Soil–Struct. Interaction*, A. A. Balkema, Rotterdam, 1984, pp. 3–11.

14. J. P. Wolf and J. W. Meek, 'Dynamic stiffness of foundation on layered soil half-space using cone frustums', *Earthquake Engng. Struct. Dyn.* **23**, 1079–1095 (1994).
15. G. Gazetas, 'Foundation vibrations', in H. Y. Fang (ed.), *Foundation Engineering Handbook*, Van Nostrand Reinhold, New York, 1991, pp. 553–593.
16. C. Vrettos, 'In-plane vibrations of soil deposits with variable shear modulus: I. Surface waves', *Int. J. Numer. Anal. Meth. Geomech.* **14**, 209–222 (1990).
17. C. Vrettos, 'Time-harmonic Boussinesq problem for a continuously nonhomogeneous soil', *Earthquake Engng. Struct. Dyn.* **20**, 961–977 (1991).
18. C. Vrettos, 'Elastic settlement and rotation of rectangular footings on nonhomogeneous soil', *Géotechnique* **48**, 703–707 (1998).
19. H. L. Wong and J. E. Luco, 'Dynamic response of rigid foundations of arbitrary shape', *Earthquake Engng. Struct. Dyn.* **4**, 579–587 (1976).
20. S. A. Savidis and T. Richter, 'Dynamic interaction of rigid foundations', *Proc. 9th Int. Conf. Soil Mech. Found. Eng.*, Tokyo, 1977, Vol. 2, pp. 369–374.
21. W. Sarfeld, 'Numerische Verfahren zur dynamischen Boden-Bauwerk Interaktion', *Veröffentl. des Grundbauinstitutes der Technischen Universität Berlin*, Heft 22, 1994.
22. C. Vrettos, 'Influence of soil stiffness increase with depth on the contact pressure of rigid plates', in R. Katzenbach and U. Arslan (eds), *Proc. Int. Conf. Soil-Structure Interaction in Urban Civil Engineering*, Darmstadt, 1998, Vol. 2, pp. 437–446.
23. L. Gaul, 'Dynamische Wechselwirkung eines Fundamentes mit dem viskoelastischen Halbraum', *Ingenieur-Archiv* **46**, 401–422 (1977).

